JOURNAL OF GUIDANCE, CONTROL, AND DYNAMICS
Vol. 40, No. 5, May 2017

Dynamics and Precision Control of Uncertain Tumbling Multibody Systems

Prasanth B. Koganti* and Firdaus E. Udwadia†
University of Southern California, Los Angeles, California 90089

DOI: 10.2514/1.G002212

This paper deals with the precision control of tumbling multibody systems with uncertainties present in the descriptions of their mathematical models. A generic tumbling multibody system consisting of a rigid body with internal degrees of freedom is used. A two-step control methodology is developed. First, a nominal system is conceived that best approximates the actual physical system. An analytical dynamics-based control methodology is used to obtain the nominal control force that ensures that this nominal system satisfies the control requirements. This is done using the control methodology proposed by Udwadia ("Optimal Tracking Control of Nonlinear Dynamical Systems," *Proceedings of the Royal Society of London, Series A: Mathematical and Physical Sciences*, Vol. 464, 2008, pp. 2341–2363). Second, an additional compensating generalized control force is designed to ensure that the actual controlled (uncertain) system tracks the trajectories of the nominal system so that the control requirements are also met by the actual system. This paper deals primarily with the second step and its combination with the first. Uncertainties in both the description of the system as well as the forces acting on it are considered. No linearizations or approximations are made in either of the steps, and the full nonlinear dynamical system is considered. The efficacy of the control methodology is demonstrated by applying it to two tumbling uncertain multibody dynamical systems.

I. Introduction

THIS paper deals with the dynamics and precision control of a generic multibody tumbling system with internal degrees of freedom when uncertainty is present in its description. It extends the control methodology developed in [1] in which a closed-form control was provided to accurately control a tumbling multibody dynamical system for which the mathematical model is assumed to be accurately known (i.e., the nominal system). Here, it is assumed that both the description of and the given forces acting on the actual tumbling multibody system are only imprecisely known; an estimate of the extent of the uncertainties involved is available. In real-life situations, uncertainty estimates can themselves be unreliable and prone to considerable error. To circumvent this problem, it is further shown that the control methodology developed herein to compensate for these uncertainties is relatively insensitive to errors in the uncertainty estimates.

Although the research reported on tumbling bodies is limited, there is a significant body of research available in the literature for the uncertain attitude control problem for which various methods ranging from simple proportional, integral, derivative (PID) control techniques to sophisticated higher-order sliding-mode control techniques have been investigated. In the following, we present a few representative results. Reference [2] uses a passivity approach to control the attitude of a rigid body when angular velocity is unknown. Reference [3] investigates the use of PID control approaches for robust tracking of spacecraft attitude. Reference [4] introduces an adaptive variable-structure control approach for attitude control of a flexible spacecraft with dead-zone and saturation nonlinearity in input. Reference [5] investigates the tracking control problem of unmanned aerial vehicles, and control is obtained that can track both the attitude angles and angular velocities using a two-loop sliding-mode control scheme in which the scaling factor is obtained using fuzzy rules to avoid chattering problems. Reference [6] employs a radial basis function neural network (RBFNN) to approximate the system uncertainty, and control is designed to control the attitude of a near-space vehicle based on the output of the RBFNN and sliding-mode observers. Reference [7] provides a robust nonlinear attitude control method for quadrotors with uncertain parameters. The control consists of a nominal control that is linear in nature and a compensating control obtained using robust filters. Reference [8] uses model reference adaptive control in which the parameters describing the system are assumed to be uncertain; the approach ensures that the control requirements are met asymptotically. Reference [9] investigates the use of the Kalman filter for estimating the uncertain dynamics of tumbling bodies, and optimal trajectories are generated for a service robot to capture a tumbling body.

This paper develops a completely different control philosophy from those cited previously. As in [1], the central idea is to frame the modeling constraints and the control requirements that are placed on the multibody tumbling system as a set of constraints imposed on it. Control of the uncertain multibody tumbling system is achieved in two steps. In the first step, a nominal system, which is the best available description of the uncertain system, is conceived. This nominal system is then controlled using the analytical dynamics approach developed and demonstrated in [1]. The methodology yields, in closed form, the exact (generalized) control force required to enforce the modeling and control constraints that ensure that the nominal system asymptotically satisfies the control requirements. The nominal control force simultaneously minimizes a quadratic control cost at each instant of time [10–14].

Next, a closed-form expression for an additional compensating control force is obtained so that the actual uncertain system tracks (mimics) the behavior of the tumbling nominal system to within user-specified tolerances, thereby making the actual system behave as though there were no uncertainty in the description of the nominal system. The development of this compensating controller and its use in conjunction with the closed-form control obtained for the nominal system are the primary contributions of this paper.

The general idea behind the methodology for the second step, which uses a generalized sliding-mode surface, was first proposed in [15], and it has been used in various forms suitably adapted for different problems [16,17]. With the use of a smooth function in place of a signum function, the approach avoids chattering and other problems associated with sliding-mode control reported in the literature [18–21]. The approach proposed in [15] can use any user-prescribed continuous, odd, monotonic increasing function in lieu of the signum function; this paper uses a function that is linear in the

Received 7 May 2016; revision received 7 October 2016; accepted for publication 9 October 2016; published online 10 March 2017.

*Department of Aerospace and Mechanical Engineering.
†Professor, Aerospace and Mechanical Engineering, Civil Engineering, Mathematics, and Information and Operations Management; fudwadia@gmail.com.

sliding variable. The approach presented in [15], though more flexible, has the drawback that the maximum allowed uncertainty in the generalized mass matrix is a function of the number of degrees of freedom; hence, the methodology is limited in handling large uncertainties (in generalized mass) in large-scale systems with many degrees of freedom. The approach developed herein does not have this limitation and is suitable for larger systems. The sliding-mode control presented in [16] also takes any user-prescribed smooth, odd, monotonic increasing function as a control design input but is applicable only for dynamical systems that do not have uncertainty in the generalized mass. Though the current approach does not have this added flexibility (of being able to choose a user-prescribed function of the sliding variable) as in [15,16], it is applicable to larger systems that have significant uncertainties in both the generalized mass matrix and the generalized forces. More important, it has a significant practical advantage: the closed-form additional compensating (generalized) control force is relatively insensitive to errors in the estimated uncertainties.

No approximation and/or linearizations are made throughout, and the exact nonlinear tumbling dynamics of the uncertain multibody system is used. For purposes of comparison, the two illustrative examples of tumbling–vibrating multibody systems previously considered in [1] are revisited: now with uncertain descriptions of both the parameters involved in specifying the system and the forces acting on it. The efficacy, simplicity, and ease of use of the control methodology are demonstrated through these examples.

II. Nominal System and its Precision Control

The generic uncertain multibody tumbling system with internal moving parts under consideration is depicted in Fig. 1. It is assumed to comprise the following two components (see Fig. 1a).

1) The first component is a rigid body B of mass m_B and a (rigid) rod R of mass m_R that is fixed to the body B. The center of mass of the composite rigid body (denoted hereafter as BR) is located at C (see Fig. 1a). The coordinate axes of the body-fixed coordinate frame xyz, for which the origin is chosen to coincide with C, lie along the principal axes of inertia of BR. The direction of the axis of the rod R is specified by the unit vector a for which the components in the body-fixed coordinate frame are the constants a_1, a_2, and a_3, respectively. The coordinates of C in the inertial coordinate frame XYZ are denoted by (X_c, Y_c, Z_c). The vector from C to a suitable point O' on the rod R is the three-vector d, for which the components in the xyz frame are the constants d_1, d_2, and d_3, respectively (see Fig. 1a).

2) The second component is a set of n discrete masses m_i, $i = 1, 2, \ldots, n$, that slide along the rod, with each mass connected to its nearest neighbor by linear and nonlinear spring elements (see Fig. 1b). The position of the masses measured from O' along the rod R are denoted by p^i, $i = 1, 2, \ldots, n$. As shown in Fig. 1b, the spring element k_{i+1} connecting mass m_i to mass m_{i+1} is assumed, for simplicity, to consist of a linear elastic spring element with stiffness k^l_{i+1} in parallel with a cubically nonlinear elastic spring element with stiffness k^n_{i+1}. The equilibrium positions of the discrete masses are given by p^i_e, $i = 1, 2, \ldots, n$, as measured along the rod R from O'.

The generic uncertain multibody tumbling system with internal degrees of freedom described previously has practical significance in studying phenomena like liquid sloshing in rockets, capture and refurbishing of space debris, and control of tumbling microrobots. In this paper, for simplicity, we assume that the multibody tumbling system moves in a constant gravity field with a downward (uncertain but constant) acceleration g.

The rigid body BR has six degrees of freedom, and each point mass has one degree of freedom. Thus, a total of $n + 6$ coordinates are required to describe the configuration of the system. However, in what follows, an additional coordinate will be used to describe the composite system's configuration, and its rotational motion will be described by four quaternions. The mass of BR (bodies B and R) is denoted by m_{BR}, and its mass moment of inertia matrix with respect to the body-fixed frame located at C (for which the directions are along the principal axes of inertia of BR) is denoted by $J = \mathrm{diag}(J_x, J_y, J_z)$.

As mentioned previously, the nominal system is a description of the system (the parameters involved, the forces acting, etc.) based on the best available knowledge of the actual (physical) system in which the parameters (and the forces acting) are only known imprecisely. The equation of motion of the controlled nominal system is given by

$$M_{(n)}\ddot{q}_{(n)} = Q_{(n)} + Q^C \tag{1}$$

where $q_{(n)} = [X_c, Y_c, Z_c, u^T, p^T]^T$ is the generalized displacement vector consisting of the three coordinates of the center of mass of the tumbling body BR with respect to an inertial frame XYZ, the quaternion $u = [u_0, u_1, u_2, u_3]^T$ represents the attitude of the body BR, and the vector $p = [p_1, p_2, \ldots, p_n]$ gives the positions of the masses along the rod R relative to reference point O' (see Fig. 1). In the preceding, the subscript (n) on various quantities indicates the nominal system. $M_{(n)}$ and $Q_{(n)}$ are the generalized mass matrix and the generalized force vector acting on the unconstrained dynamical system. They are explicitly given in [1] by

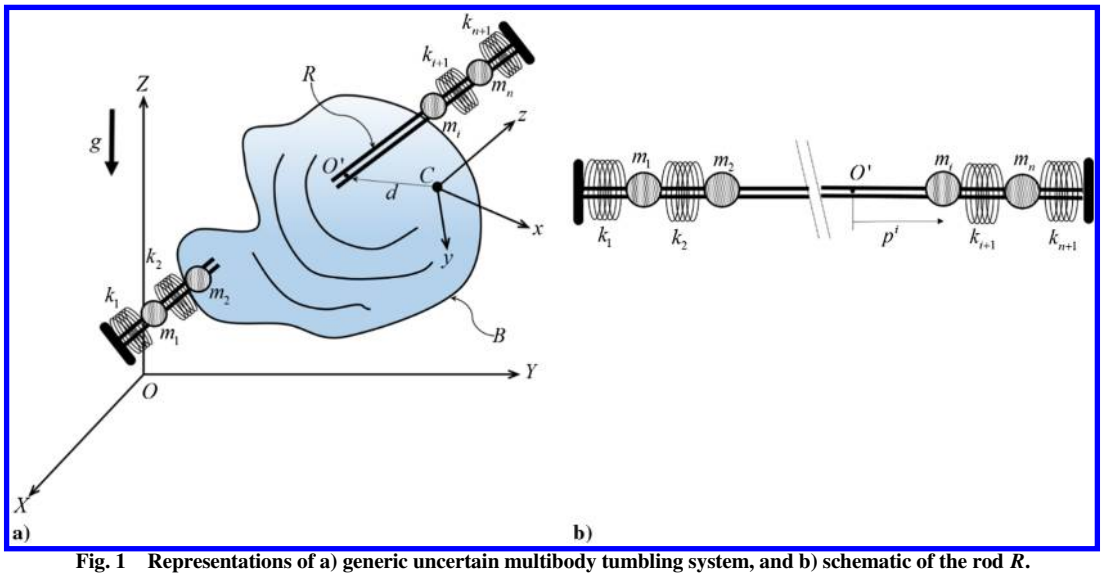

Fig. 1 Representations of a) generic uncertain multibody tumbling system, and b) schematic of the rod R.

$$M_{(n)} = \begin{bmatrix} \{m_{BR} + m^T 1_n\} I_3 & \{m^T p\} L_a + \{m^T 1_n\} L_d & (Sa) m^T \\ \{m^T p\} L_a^T + \{m^T 1_n\} L_d^T & H^T J H + \{(p \circ m)^T p\} L_a^T L_a + A_d & L_a^T Sa (p \circ m)^T + L_d^T Sa m^T \\ m(Sa)^T & (p \circ m)(Sa)^T L_a + m(Sa)^T L_d & \{(Sa)^T Sa\} \mathrm{diag}(m) \end{bmatrix} \tag{2}$$

where

$$A_d = \{m^T p\}(L_a^T L_d + L_d^T L_a) + \{m^T 1_n\} L_d^T L_d$$

$$Q_{(n)} = \begin{bmatrix} -2\{m^T \dot{p}\} L_a \dot{u} - (\{m^T p\} \dot{L}_a + \{m^T 1_n\} \dot{L}_d) \dot{u} - g(m_{BR} + \{m^T 1_n\}) e_3 \\ -2\dot{H}^T J H \dot{u} - 2\{(p \circ m)^T \dot{p}\} L_a^T L_a \dot{u} - \{(p \circ m)^T p\} L_a^T \dot{L}_a \dot{u} - g\{p^T m\} L_a^T e_3 + B_d \\ -\{(Sa)^T \dot{L}_a \dot{u}\}(p \circ m) - 2\{(Sa)^T L_a \dot{u}\}(\dot{p} \circ m) - \{(Sa)^T \dot{L}_d \dot{u}\} m + F^S - g\{(Sa)^T e_3\} m \end{bmatrix} \tag{3}$$

where

$$B_d = -(2\{m^T \dot{p}\} L_d^T L_a + \{m^T p\} L_a^T \dot{L}_d + \{m^T p\} L_d^T \dot{L}_a + \{m^T 1_n\} L_d^T \dot{L}_d) \dot{u} - g\{m^T 1_n\} L_d^T e_3$$

and

$$F_i^S = -k_i^l (p^i - p^{i-1} - p_e^i + p_e^{i-1}) - k_i^n (p^i - p^{i-1} - p_e^i + p_e^{i-1})^3 + k_{i+1}^l (p^{i+1} - p^i - p_e^{i+1} + p_e^{i-1}) + k_{i+1}^n (p^{i+1} - p^i - p_e^{i+1} + p_e^{i-1})^3 \tag{4}$$

For convenience, scalars are shown in curly brackets. In Eqs. (2) and (3), $m = [m_1, m_2, \ldots, m_n]^T$, 1_n is the n vector each of whose elements is unity, $e_3 = [0, 0, 1]^T$, and $p \circ m$ is the Hadamard product of vectors p and m defined as

$$p \circ m = [p_1 m_1, p_2 m_2, \ldots, p_n m_n]^T \tag{5}$$

The matrix S is the active rotation matrix given by

$$S(u) := [S_1 \; S_2 \; S_3] = \begin{bmatrix} 2u_0^2 - 1 + 2u_1^2 & 2u_1 u_2 - 2u_0 u_3 & 2u_1 u_3 + 2u_0 u_2 \\ 2u_1 u_2 + 2u_0 u_3 & 2u_0^2 - 1 + 2u_2^2 & 2u_2 u_3 - 2u_0 u_1 \\ 2u_1 u_3 - 2u_0 u_2 & 2u_2 u_3 + 2u_0 u_1 & 2u_0^2 - 1 + 2u_3^2 \end{bmatrix} \tag{6}$$

$$H := \begin{bmatrix} -2u_1 & 2u_0 & 2u_3 & -2u_2 \\ -2u_2 & -2u_3 & 2u_0 & 2u_1 \\ -2u_3 & 2u_2 & -2u_1 & 2u_0 \end{bmatrix}, \; L_i = \frac{\partial S_i}{\partial u}, \; i = 1,2,3,$$

$$L_a := \sum_{i=1}^{3} a_i L_i \text{ and } L_d := \sum_{i=1}^{3} d_i L_i \tag{7}$$

The nominal system has to satisfy the modeling unit-quaternion constraint ($\varphi_m := u^T u - 1 = 0$) that, upon two differentiations with respect to time, can be expressed as

$$A_m(q_{(n)}, \dot{q}_{(n)}, t) \ddot{q}_{(n)} = b_m(q_{(n)}, \dot{q}_{(n)}, t) \tag{8}$$

One could also use the dynamical system

$$\ddot{\varphi}_m + \delta_1 \dot{\varphi}_m + \delta_2 \varphi_m = 0, \quad \delta_1, \delta_2 > 0 \tag{9}$$

as a modeling constraint on the unconstrained system. Note that $\varphi_m(0) = 0$, and this constraint ensures that $\varphi_m \to 0$ as $t \to \infty$, thus attempting to keep $\varphi_m(t)$ close to zero. Equation (9) can also be expressed in the form given in Eq. (8).

The control requirements are cast in the form of constraints on the nonlinear dynamical system. Two types of constraints generally arise. They are of the form

$$\varphi_c(q, t) = 0 \tag{10}$$

where φ_c is an h vector, and

$$\psi_c(\dot{q}, q, t) = 0 \tag{11}$$

where ψ_c is a j vector.

We differentiate each equation in the set from Eq. (10) twice with respect to time t and each equation in the set from Eq. (11) once with respect to time. We then form the dynamical equations

$$\ddot{\varphi}_c + \mathrm{diag}(\alpha_1, \alpha_2, \ldots, \alpha_h) \dot{\varphi}_c + \mathrm{diag}(\beta_1, \beta_2, \ldots, \beta_h) \varphi_c = 0 \tag{12}$$

and

$$\dot{\psi}_c + \mathrm{diag}(\gamma_1, \gamma_2, \ldots, \gamma_j) \psi_c = 0 \tag{13}$$

in which the parameters in the diagonal matrices are chosen to be positive. Matrices that are more general than the diagonal matrices shown can also be used; but, for simplicity, we will use these here. This choice of parameters ensures that φ_c, $\psi_c \to 0$ asymptotically as $t \to \infty$.

The control requirements given by Eqs. (12) and (13) can always be expressed as

$$A_c(q_{(n)}, \dot{q}_{(n)}, t) \ddot{q}_{(n)} = b_c(q_{(n)}, \dot{q}_{(n)}, t) \tag{14}$$

Furthermore, both sets of constraints (modeling and control) given by Eqs. (8) and (14) can combined as

$$A_{(n)} \ddot{q}_{(n)} := \begin{bmatrix} A_m \\ A_c \end{bmatrix} \ddot{q}_{(n)} = \begin{bmatrix} b_m \\ b_c \end{bmatrix} := b_{(n)} \tag{15}$$

The generalized force vector Q^C [see Eq. (1)] consisting of both the constraint force required to enforce the modeling constraint (unit-quaternion requirement) as well as the control force required to enforce the control constraints is given by the fundamental equation of motion in closed form as follows [10,11]:

$$Q^C = A_{(n)}^T \left(A_{(n)} M_{(n)}^{-1} A_{(n)}^T \right)^+ \left(b_{(n)} - A_{(n)} M_{(n)}^{-1} Q_{(n)} \right) \tag{16}$$

The efficacy of this control approach for the nominal system has been demonstrated in [1] with numerical examples of a tumbling–vibrating multibody parallelepiped–rod system and a tumbling–vibrating cylinder–rod system. However, because the correct model of an actual physical system can substantially deviate from the nominal system, applying only the nominal (generalized) control force to the actual system may not lead to the controlled actual system satisfying the desired control objectives. Hence, it is necessary to use an additional compensating control force with the purpose of

controlling the actual system so that it tracks the trajectories of the nominal system. The uncertain system then behaves dynamically as though it were the nominal system; because the nominal system satisfies the desired control objectives (asymptotically), the controlled actual system will satisfy them too.

III. Precision Control of Actual Uncertain System

The equation of motion of the controlled actual (physical) system is

$$M(q)\ddot{q} = Q(q, \dot{q}) + Q^C(q_{(n)}, \dot{q}_{(n)}, t) + Q^u(q, \dot{q}, t) \tag{17}$$

where M is the positive definite, symmetric generalized (uncertain) mass matrix; and Q is the (uncertain) generalized impressed force vector acting on the actual system. Q^C is the generalized nominal control force vector that is obtained by considering the nominal system; and Q^u is the generalized additional compensating control force, yet to be found, which causes the uncertain system to dynamically behave as though it were the nominal system. The generalized control force Q^u, in a sense, compensates for the presence of uncertainties and our ignorance of the actual physical system. It should be noted that the nominal control force does not explicitly depend on the state of the actual (physical) system.

The tracking error between the controlled actual system and the nominal system is defined as

$$e(t) = q(t) - q_{(n)}(t) \tag{18}$$

and the tracking error in generalized velocity is defined as

$$\dot{e}(t) = \dot{q}(t) - \dot{q}_{(n)}(t) \tag{19}$$

A sliding surface is defined as

$$s(t) \coloneqq \dot{e}(t) + Ke(t) \tag{20}$$

where $K > 0$ is a (constant) scalar. It is easily seen that, when the controlled actual system is confined to the hyperplane $s = 0$, the tracking error converges to zero asymptotically; hence, the control objectives are satisfied asymptotically (because the nominal system satisfies the control objectives asymptotically and the controlled actual system tracks the trajectory of the nominal system exactly). However, control methods capable of driving systems to this hyperplane in finite time are discontinuous and have performance issues. To avoid the problems associated with discontinuous control methods, we intend to use a smooth control that will ensure that the system stays within a region Ω_ε around this hyper plane, defined as

$$\Omega_\varepsilon \coloneqq \{s \in R^n \,|\, \|s\| \leq \varepsilon\} \tag{21}$$

In the preceding, $\varepsilon > 0$ is a scalar control design parameter that can be chosen so that the controlled actual system satisfies user-prescribed bounds on the error in tracking the nominal system. Throughout the paper, we use $\|\cdot\|$ to denote the L_2 norm. In what follows, the arguments of the various quantities are suppressed for brevity, unless required for clarity.

It should be noted that, at time $t = 0$, the nominal system and the actual system have the same generalized displacement and velocity: $e(0) = \dot{e}(0) = 0$. Hence, at time $t = 0$, the system is inside the region Ω_ε.

Defining

$$\delta\ddot{q} = M^{-1}(Q + Q^C) - M_{(n)}^{-1}(Q_{(n)} + Q^C) \tag{22}$$

and assuming that the following two estimates

$$\lambda_{\min} \leq \lambda_i, \quad \forall\ i \tag{23}$$

where λ_i are eigenvalues of the matrix $M^{-1}(q)$, and

$$\beta > \frac{\|\delta\ddot{q}\| + K\|\dot{e}\|}{\lambda_{\min}}, \quad \forall\ t \tag{24}$$

are available to us, we have the following result.

Result 1: For a given user-prescribed value of ε, the additional compensating control force Q^u defined by

$$Q^u = -\beta(s/\varepsilon) \tag{25}$$

ensures that the controlled actual uncertain (physical) system for which the equation of motion is described by Eq. (17) always stays within the region Ω_ε defined by Eq. (21).

Proof: Considering the Lyapunov function

$$V = \frac{1}{2}s^T s \tag{26}$$

its rate of change along the trajectories of the controlled actual system is

$$\dot{V} = s^T \dot{s} \tag{27}$$

On differentiating Eq. (20) with respect to time, we get

$$\dot{s} = \ddot{e} + K\dot{e} \tag{28}$$

Noting Eqs. (1), (17), and (19),

$$\ddot{e} = M^{-1}(Q + Q^C + Q^u) - M_{(n)}^{-1}(Q_{(n)} + Q^C) = \delta\ddot{q} + M^{-1}Q^u \tag{29}$$

On substituting Eq. (29) in Eq. (28), we obtain

$$\dot{s} = \delta\ddot{q} + M^{-1}Q^u + K\dot{e} \tag{30}$$

Thus, Eq. (27) is simplified as

$$\dot{V} = s^T(\delta\ddot{q} + M^{-1}Q^u + K\dot{e}) \tag{31}$$

On substituting Q^u from Eq. (25), we obtain

$$\dot{V} = s^T\delta\ddot{q} - \frac{\beta}{\varepsilon}s^T M^{-1}s + Ks^T\dot{e} \tag{32}$$

Because M^{-1} is positive definite, all its eigenvalues are real and because of relation (23), the inequality $s^T M^{-1}s \geq \lambda_{\min}\|s\|^2$ holds at all times. Thus, we can find the upper bound of $\dot{V}$ as

$$\dot{V} \leq \|s\|\|\delta\ddot{q}\| - \frac{\beta}{\varepsilon}\lambda_{\min}\|s\|^2 + K\|s\|\|\dot{e}\| \tag{33}$$

We can further simplify the preceding inequality as

$$\dot{V} \leq \|s\|\left(\|\delta\ddot{q}\| - \frac{\beta}{\varepsilon}\lambda_{\min}\|s\| + K\|\dot{e}\|\right) \tag{34}$$

outside the region Ω_ε, $\|s\|/\varepsilon > 1$. Rewriting Eq. (34), when $\|s\|/\varepsilon > 1$, we obtain

$$\dot{V} < -\|s\|\lambda_{\min}\left(\beta - \frac{\|\delta\ddot{q}\| + K\|\dot{e}\|}{\lambda_{\min}}\right) < 0 \tag{35}$$

where the last inequality follows from relation (24). Applying Lyapunov's stability theorem, we conclude that Ω_ε is an attracting region for the controlled actual system. Specifically, any trajectory that starts inside the region Ω_ε stays inside it for all future time. Because the actual system starts inside the region Ω_ε at time $t = 0$ as mentioned before, the trajectory of the actual system always stays inside Ω_ε. □

Remark 1: An estimate of β [see relations (23) and (24)] is required to determine the additional (generalized) compensating control Q^u given in Eq. (25). Its value depends on an estimate of the extent of uncertainty present in the actual uncertain system as compared with the nominal system chosen to describe it. However, overestimates of the value of β do not appear to result in a larger additional control force Q^u (as shown later in Result 3). In fact, the magnitude of Q^u, roughly speaking, remains about the same even if β is overestimated by a factor of three or more.

Remark 2: The value of ε is user-specified and can be made arbitrarily small. Theoretically, it can be chosen to meet any desired tracking-error tolerance. However, from a practical standpoint, for extremely small values of ε, computation times could become large, depending on the error tolerances used when performing the numerical integration.

Result 2: When the controlled actual system is restricted to stay within the region Ω_ε, the errors in tracking the nominal system are bounded by

$$|e_i| \le \frac{1}{K}\varepsilon, \quad i = 1, 2, \ldots, n \tag{36}$$

and

$$\left|\dot{e}_i\right| \le 2\varepsilon, \quad i = 1, 2, \ldots, n \tag{37}$$

Proof: Although this result can also be obtained through heavier mathematical machinery, we prefer to use the following more elementary approach. Inside the region Ω_ε, $\|s\| \le \varepsilon$, and hence the inequality

$$|s_i| \le \varepsilon, \quad i = 1, 2, \ldots, n \tag{38}$$

holds for at all time. Using Eq. (20), relation (38) can be expanded as

$$|\dot{e}_i + Ke_i| \le \varepsilon, \quad i = 1, 2, \ldots, n \tag{39}$$

From Eq. (39), we observe that relation (37) follows from relation (36) as

$$||\dot{e}_i| - K|e_i|| \le |\dot{e}_i + Ke_i| \le \varepsilon$$

and hence

$$|\dot{e}_i| \le \varepsilon + K|e_i| \le 2\varepsilon \tag{40}$$

So, we focus on proving relation (36). Equation (39) can be alternatively written as

$$-\varepsilon \le \dot{e}_i + Ke_i \le \varepsilon, \quad i = 1, 2, \ldots, n \tag{41}$$

or

$$-\varepsilon - Ke_i \le \dot{e}_i \le \varepsilon - Ke_i, \quad i = 1, 2, \ldots, n \tag{42}$$

Considering e_i as a dynamical system, if we can prove that $e_i\dot{e}_i < 0$ outside the region defined by relation (36), then we can conclude that relation (36) holds true because $e_i\dot{e}_i$ is the derivative of $(1/2)e_i^2$, which is a Lyapunov function for the e_i dynamical system and, at time $t = 0$, $e_i = \dot{e}_i = 0$.

If

$$e_i > \frac{1}{K}\varepsilon > 0$$

then

$$\varepsilon - Ke_i < 0 \tag{43}$$

Hence, by Eq. (42), $\dot{e}_i < 0$; so, $e_i\dot{e}_i < 0$. If $e_i < -(1/K)\varepsilon < 0$, then

$$-\varepsilon - Ke_i > 0 \tag{44}$$

and, by Eq. (42), $\dot{e}_i > 0$; and again, $e_i\dot{e}_i < 0$. Thus, we can conclude that relation (36) holds true, and so does relation (37) by extension. □

Remark 3: The total (generalized) control force applied on the uncertain system is $Q^C + Q^u$. Because the actual system tracks the trajectories of the nominal system to any user-prescribed precision (see Result 2), the actual system also satisfies the constraints, and hence the control requirements to the corresponding precision.

From Eq. (25), we have the following for 1) any value of β satisfying relation (24) and 2) any chosen value of ε:

$$Q^u = -\beta\frac{s}{\varepsilon}, \quad \beta > 0 \tag{45}$$

A value of β that satisfies relation (24) will be referred to as a permissible value for the control design. The feasibility of the control methodology proposed here thus depends on the availability of a permissible β. However, accurate estimates of the right-hand side of relation (24) might not, and generally speaking would not, be available. In such cases, the following result shows that conservative overestimates of (permissible values) of β will do, and they will not cause the additional compensating control force to be significantly different.

Result 3: Having chosen 1) a value of $\varepsilon = \varepsilon_0$, and 2) a permissible value $\beta = \beta_0$ for the design of the compensating control, the norm of the additional compensating control force Q^u is relatively insensitive to use of a larger value (overestimate) of $\beta = \beta_1 > \beta_0$ as long as $\beta_1/\beta_0 = O(1)$.

Proof: For any permissible value of β, $\|s\|/\varepsilon \le 1$ for any chosen value of ε. The worst situation is when $\|s\|/\varepsilon = 1$, so that $\|s(t)\|/\varepsilon = O(1)$ as $t \to \infty$. By Eq. (45), then

$$\|Q^u\| = \beta\frac{\|s\|}{\varepsilon} = O(\beta) \tag{46}$$

for any permissible value of β and any given value of ε.

For a permissible value $\beta = \beta_0$ and a user-specified value $\varepsilon = \varepsilon_0$ used in the control design, the additional compensating control Q_0^u, from Eq. (46), is such that

$$\|Q_0^u\| = O(\beta_0) \tag{47}$$

and

$$\|s\|/\varepsilon_0 = O(1) \tag{48}$$

The value of β_0 used in the control design needs to be estimated, and it depends on our level of knowledge (ignorance) of the actual physical system. But, for a real-life system, the extent of this knowledge (ignorance) regarding the actual system (vis-à-vis the nominal system that is used) is usually difficult to exactly assess, thus making the value of β_0 that is to be used itself uncertain. Hence, if an overestimate $\beta_1 > \beta_0$ is used instead of β_0 in the control design in order to be conservative, then from relation (45) (because β_1 is a permissible value of β)

$$\|Q_1^u\| = \beta_1\frac{\|s\|}{\varepsilon_0} = \beta_0\frac{\beta_1}{\beta_0}\frac{\|s\|}{\varepsilon_0} = \beta_0\frac{\|s\|}{\varepsilon_1} \tag{49}$$

where $\varepsilon_1 = \varepsilon_0(\beta_0/\beta_1) < \varepsilon_0$. Furthermore, if $\beta_1/\beta_0 = O(1)$ and, by Eq. (48), $\|s\|/\varepsilon_0 = O(1)$, we obtain

$$\frac{\|s\|}{\varepsilon_1} = \frac{\beta_1}{\beta_0}\frac{\|s\|}{\varepsilon_0} = O(1)$$

Equation (49) informs us that 1) by increasing the value of β from β_0 to β_1 we have effectively reduced the value of ε from ε_0 to ε_1; and 2) if $\beta_1/\beta_0 = O(1)$, then $\|s\|/\varepsilon_1 = O(1)$, and the additional compensating control force Q_1^u when using a value of $\beta = \beta_1 > \beta_0$ is such that

$$\|Q_1^u\| = \beta_0 \frac{\|s\|}{\varepsilon_1} = \beta_0 O(1) = O(\beta_0) = O(\|Q_0^u\|) \qquad (50)$$

where the first equality follows from Eq. (49) and the last follows from Eq. (47).

Thus, use of a larger permissible value of β does not significantly increase the magnitude of the compensating control force. □

IV. Numerical Examples

The first example considered is that of a rectangular parallelepiped (body B) with a cylindrical rod attached perpendicular to its surface. Two discrete masses slide smoothly along the rod R. The masses are connected to one another and to the ends of the rod by linear spring elements in parallel with nonlinear cubic spring elements. The second example consists of a hollow cylinder B with a coaxial rod R. Five discrete masses slide along the rod R. Each mass is connected to its nearest neighbors (and to the end points of the rod) by linear and nonlinear spring elements, in parallel. The first example demonstrates precision control of uncertain asymmetrical multibody tumbling–vibrating systems; the second demonstrates control of uncertain symmetrical systems.

A. Example 1

Figure 2 shows the dynamical system under consideration. First, we describe the properties of the nominal system, which is our best description (estimate) of the actual system and its parameters. Next, we imagine that the actual (unknown and uncertain) system is picked out of an ensemble of systems. To demonstrate the methodology used in this paper, we proceed to list the parameter values of one such actual system picked from such an ensemble, followed by the control objectives imposed on it. Lastly, we give the specifications of the compensating controller.

1. Nominal System

The dimensions of the rigid aluminum (density of 2.7×10^3 kg/m^3) block B are $10 \times 6 \times 2$ m. A rigid 16-m-long aluminum cylindrical rod R with a radius of 1 m is erected at one corner perpendicular to the surface of the parallelepiped. The mass of BR (body B and rod R) is $m_{BR(n)} = 4.597 \times 10^5$ kg. The X axis of the XYZ inertial frame is pointed along the 10 m edge of the parallelepiped B, and the Z axis is pointed vertically upward (see Fig. 2). The xyz body-fixed frame has its origin C at the center of mass of BR, and the body-fixed coordinates are along the principal axes of inertia of BR. The moment of inertia matrix of BR is given by $J_{(n)} = 10^7 \times \text{diag}(1.3626, 1.5333, 0.3848)$ kg · m^2. The reference point O' on the rod is located at the center of the circle where the rod R meets the parallelepiped B. The vector from point C to the reference point O' is $d_{(n)} = [3.2616, 1.4196, -0.1623]^T$ m. The unit vector a in the xyz coordinate frame along the direction of the rod is $a_{(n)} = [-0.3985, -0.1481, 0.9051]^T$. The nominal value of the (constant) acceleration due to gravity is taken to be $g_{(n)} = 9.81$ m/s^2.

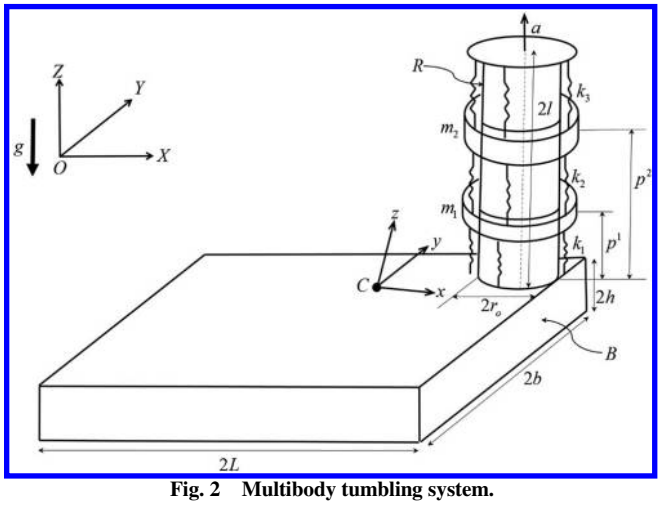

Fig. 2 Multibody tumbling system.

The masses of the sleeves (discrete masses) sliding along the rod are $m_1 = 5 \times 10^5$ kg and $m_2 = 4 \times 10^5$ kg. The linear spring elements connecting the masses have stiffnesses $k^l_{(n),1} = 6$ mN/m, $k^l_{(n),2} = 7.5$ mN/m, and $k^l_{(n),3} = 3$ mN/m; the stiffnesses of the nonlinear cubic spring elements are $k^n_{(n),1} = 0.55$ mN/m^3, $k^n_{(n),2} = 0.3$ mN/m^3, and $k^l_{(n),3} = 0.2$ mN/m^3. The equilibrium positions (in meters) of the discrete masses measured along R from the reference point O' are $p_e = [4, 12]^T$. The moment of inertia (kilograms-meter square) of the discrete masses m_1 and m_2 about their principal axes are $J_i = \text{diag}(m_i r_0^2/2, m_i r_0^2/2, m_i r_0^2)$, $i = 1, 2$, with values

$$J_{1,(n)} = 10^5 \times \text{diag}(2.5, 2.5, 5),$$
$$J_{2,(n)} = 10^5 \times \text{diag}(2, 2, 4) \text{ kg} \cdot \text{m}^2 \qquad (51)$$

Because the masses m_1 and m_2 are not considered as point masses, in order to include their rotational kinetic energy, the matrix $J = J_{BR}$ is modified to

$$J = J_{BR} + \sum_{i=1}^{2} P_i^T J_i P_i \qquad (52)$$

where the mass moment of inertia of body BR is explicitly denoted by J_{BR}, and P_i are rotation matrices. Here, the rotation matrix $P_1 = P_2 = P$ is [1]

$$P = \begin{bmatrix} 0.9171 & -0.0765 & 0.3912 \\ 0.0113 & 0.9860 & 0.1664 \\ -0.3985 & -0.1481 & 0.9051 \end{bmatrix} \qquad (53)$$

The initial position of the center of mass C of body BR is taken to be the origin O, so that $R(0) = [0, 0, 0]^T$ m, and its initial velocity is taken to be $\dot{R}(0) = [1, 2, 20]^T$. The initial orientation of the body is obtained by rotating it about the unit vector $v = 1/\sqrt{3} \times [1, 1, 1]^T$ in the inertial XYZ frame through an angle $\theta = \pi/3$ so that the quaternion at initial time is $u(0) = [0.8034, 0.1600, 0.4272, 0.3828]^T$. The initial angular velocity ω about the principal axis through C is taken to be the three-vector $\omega(0) = [1, -1, 0.5]^T$ so that $\dot{u}(0) = [0.0379, 0.6999, -0.2503, -0.0927]^T$. The initial positions $p^i_{(n)}$ of the discrete masses measured along the rod R from the reference point O' are $p(0) = [5, 11]^T$, and their initial velocities are $\dot{p}(0) = [-0.4, 0.3]^T$.

2. Actual System

The actual uncertain system has parameters and given forces that are unknown to the person modeling the system. We imagine that the actual system belongs to an ensemble of systems and that a candidate from this ensemble is picked (realized) in actuality. For purposes of demonstrating our methodology, we provide the parameters of such a system that is picked.

The mass of BR in the actual system is $m_{BR} = 4.826 \times 10^5$ kg. Its moment of inertia along the principal axes is $J = 10^7 \times \text{diag}(0.3846, 1.2126, 1.3482)$ kg · m^2. The actual masses of the sleeves are $m_1 = 5.26 \times 10^5$ kg and $m_2 = 3.735 \times 10^5$ kg Their moments of inertia about their principal axes are $J_1 = 10^5 \times \text{diag}(2.6303, 2.6303, 5.2605)$ and $J_2 = 10^5 \times \text{diag}(1.8676, 1.8676, 3.7353)$ kg · m^2. The linear spring elements connecting the masses have stiffnesses $k^l_1 = 6.044$ mN/m, $k^l_2 = 7.636$ mN/m, and $k^l_3 = 2.94$ mN/m; and the stiffnesses of the nonlinear cubic spring elements are $k^n_1 = 0.551$ mN/m^3, $k^n_2 = 0.319$ mN/m^3, and $k^l_3 = 0.204$ mN/m^3. The initial conditions and other parameters are the same as those for the nominal system.

Thus the mass of BR in the actual system differs from that used in the nominal system by approximately 5%, the moments of inertia differ by about 12%, the values of the discrete masses differ by about 6%, the

values of the stiffnesses of the linear spring elements differ by 2%, and the values of the stiffnesses of the cubic spring elements differ by 6%.

The gravitational constant is also assumed to be uncertain, and its actual value is taken to be $g = 9.73\ \mathrm{m/s^2}$.

3. Control Objectives

The system is controlled such that the tumbling motion of the composite body tracks the desired angular velocities and the motion of the internal masses tracks desired trajectories.

1) The positions $p^i(t)$ of the vibrating masses along the rod relative to the reference point O' are required to track the desired trajectories $\bar{p}^i(t)$, which involve harmonic oscillations around the equilibrium positions p_e^i with amplitude l^i and frequency λ_i so that

$$\bar{p}^i(t) = p_e^i + l^i \cos(\lambda_i t), \quad i = 1, 2 \tag{54}$$

and

2) The angular velocity components ω_i of the body BR are required to track desired trajectories $\bar{\omega}_i(t)$ given by

$$\bar{\omega}_i(t) = b_i \cos(\sigma_i t), \quad i = 1, 2, \text{and } 3 \tag{55}$$

In the preceding, bars above the various quantities indicate our control requirements.

The quantities $l = [l_1, l_2]^T$, $\lambda = [\lambda_1, \lambda_2]^T$, $b = [b_1, b_2, b_3]^T$, and $\sigma = [\sigma_1, \sigma_2, \sigma_3]^T$ are user-prescribed constants. For simulation purposes, they are chosen to be

$$l = [-1, 2]^T,\ \lambda = [2\pi, \pi/2]^T,\ b = [-10, 8, 15]^T,\ \text{and } \sigma = [0, \pi, 2\pi]^T \tag{56}$$

The parameters for the constraint matrices are also chosen to be

$$\alpha_1 = \alpha_2 = 2,\ \beta_1 = \beta_2 = 12,\ \delta_1 = 0.5,\ \delta_2 = 8,\ \text{and } \gamma = 0.6 \tag{57}$$

The equations of motion of the controlled uncertain system and the nominal system given by Eqs. (17) and (1) are simultaneously integrated, with the nominal control force and the compensating control force computed using Eqs. (16) and (25).

4. Compensating Controller

The parameters for obtaining the additional compensating generalized force are chosen as $\beta = \beta_0 = 10^{12}$, $\varepsilon = 10^{-4}$, and $K = 3$. The theoretical tracking error bounds (between the actual system and the nominal system) obtained using Eqs. (36) and (37) are

$$|e_i| \le \frac{1}{K}\varepsilon = 3.3 \times 10^{-5}, \quad i = 1, 2, \ldots, 9 \tag{58}$$

and

$$|\dot{e}_i| \le 2\varepsilon = 2 \times 10^{-4}, \quad i = 1, 2, \ldots, 9 \tag{59}$$

Numerical integration is carried out using the ode15s package in MATLAB with a relative error tolerance of 10^{-12} and an absolute error tolerance of 10^{-13}. The results are presented in Figs. 3–9. Figure 3 shows the displacement time history of the discrete masses of the controlled uncertain system as well as the errors in tracking the control requirements $e_p(t) = p(t) - \bar{p}(t)$. At the end of 20 s, tracking error $e_p(20)$ is $O(10^{-8})$ m. When integration is continued

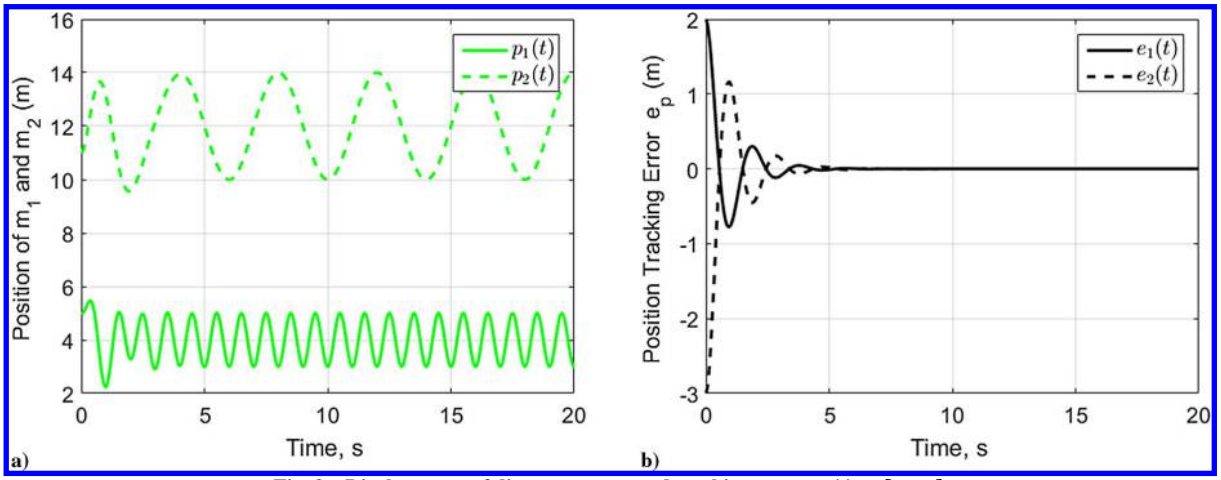

Fig. 3 Displacement of discrete masses and tracking error $e_p(t) := [e_1, e_2]$.

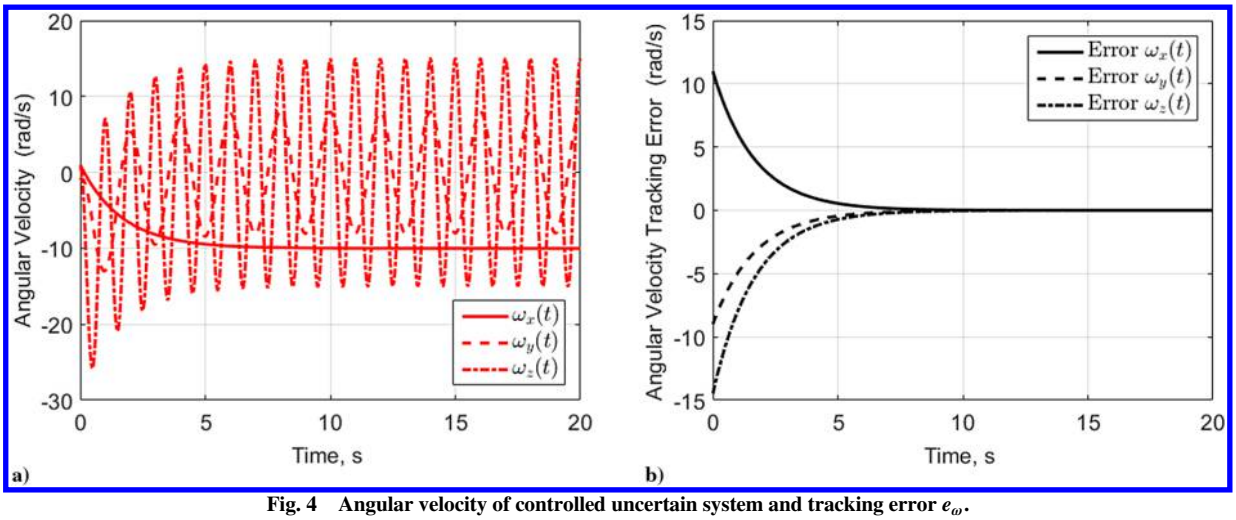

Fig. 4 Angular velocity of controlled uncertain system and tracking error e_ω.

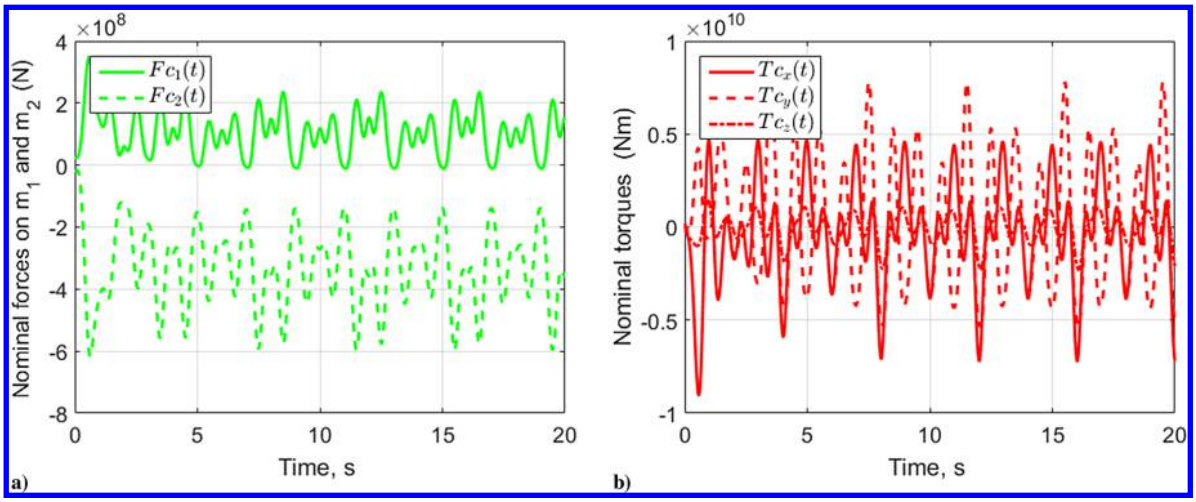

Fig. 5 Nominal control forces on discrete masses and control torques.

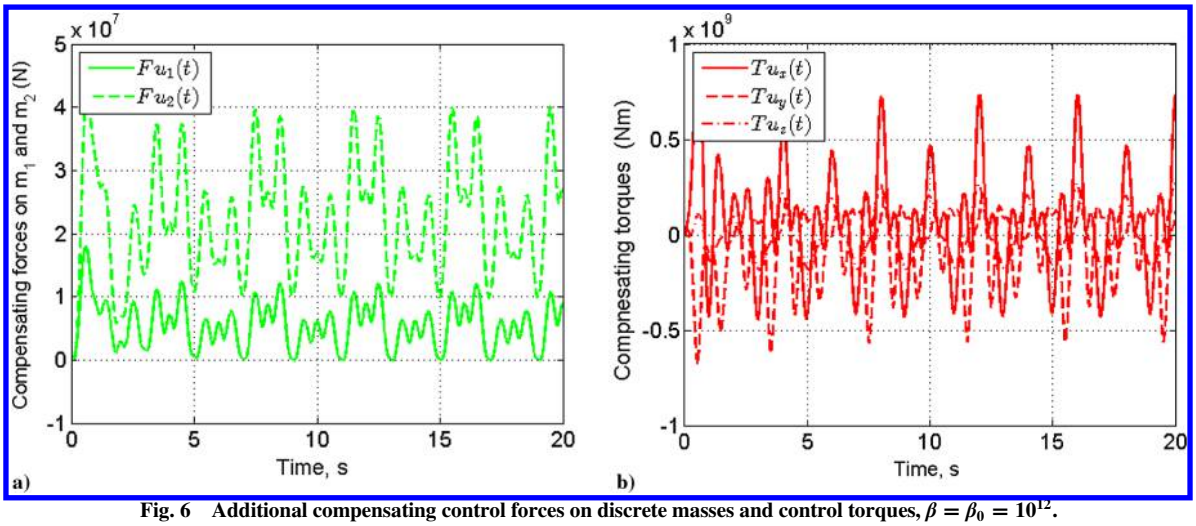

Fig. 6 Additional compensating control forces on discrete masses and control torques, $\beta = \beta_0 = 10^{12}$.

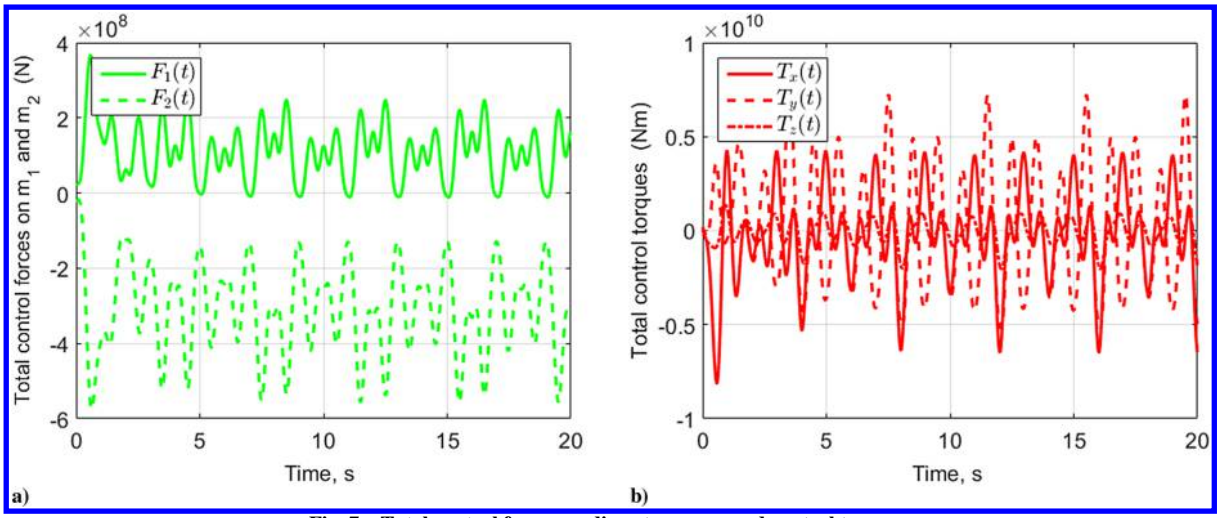

Fig. 7 Total control forces on discrete masses and control torques.

until 60 s, the tracking error at the end of 60 s, $e_p(60)$, is $O(10^{-12})$ m. Similarly, Fig. 4 shows the time history of various components of the angular velocity vector. It also shows the error in tracking the control requirements $e_\omega(t) := \omega(t) - \bar{\omega}(t)$. At the end of 20 s, the error $e_\omega(20)$ is of $O(10^{-4})$ rad/s. At the end of 60 s, the error $e_\omega(60)$ is of $O(10^{-10})$ rad/s. It should be pointed out that, at the end of 60 s, the actual tracking error $e(t) = q(t) - q_{(n)}(t)$ between the nominal and the actual systems is of $O(10^{-8})$ and the tracking error $\dot{e}(t)$ in the generalized velocity is of $O(10^{-7})$, which is much smaller than the error estimates provided by Eqs. (58) and (59).

Figure 5 shows the generalized nominal control forces to be applied to the tumbling–vibrating body so that the nominal system satisfies the control requirements. The figure on the left shows the forces on the discrete masses (denoted by Fc), whereas the one on the

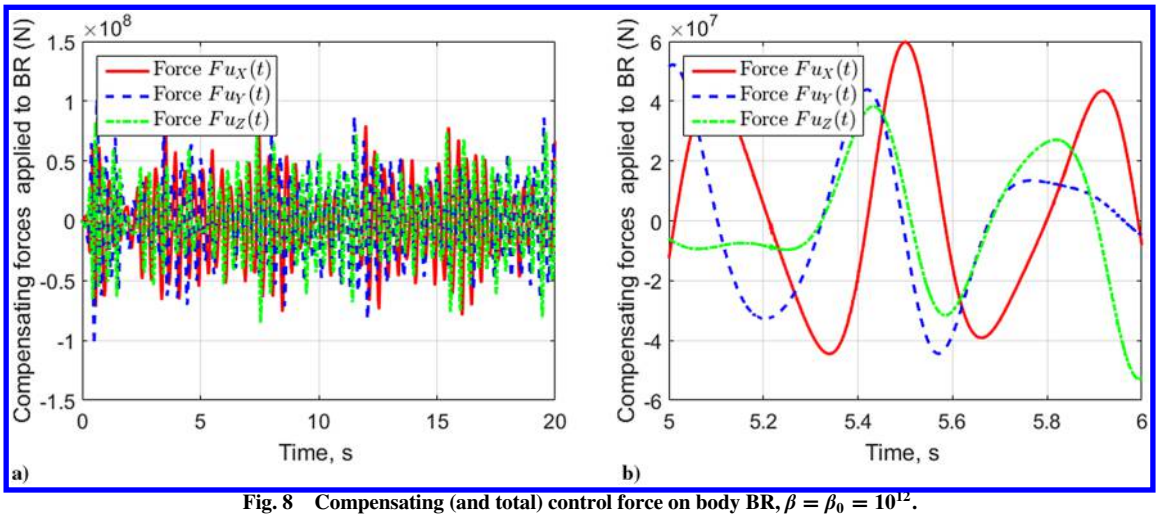

Fig. 8 Compensating (and total) control force on body BR, $\beta = \beta_0 = 10^{12}$.

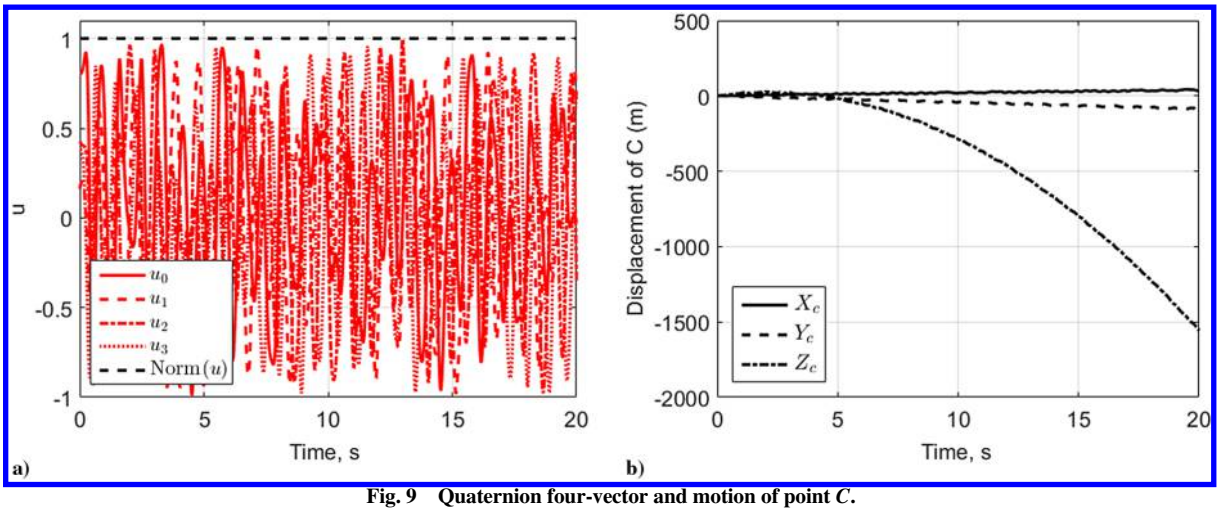

Fig. 9 Quaternion four-vector and motion of point *C*.

right shows the control torques Tc to be applied on the body BR. The nominal control force applied at C on BR is effectively zero (computationally less than 10^{-20} N throughout the interval of integration). The control torques can be computed from the generalized control forces as $Tc = (1/4)H^T Q^C_{4-7}$, where Q^C_{4-7} is the four-vector containing components of the generalized nominal control force vector Q^C from index four up to seven. These plots can be compared with similar ones in Fig. 6 that show the additional compensating control forces on the discrete masses, Fu, and the compensating control torques on the body BR, Tu. We note that the additional compensating (generalized) control forces are about an order of magnitude less than the nominal forces. The total control force, which is the sum of the nominal control force Q^C and the compensating generalized control force Q^u, causes the trajectories of the controlled uncertain system to closely track the trajectories of the nominal system so that the controlled uncertain system behaves as though it were the nominal system: that is, as though it were the nominal system with no uncertainties involved. The total control forces on the discrete masses and the control torques on the body BR are shown in Fig. 7.

Because it is assumed that there is uncertainty in the gravitational constant g, the additional compensating control forces on the body BR cannot be zero because the center of mass C (of BR) of the actual system, which is moving under the uncertain value of g (taken to be 9.73 m/s^2), has to track the corresponding center of mass C of the nominal system, which is moving under the nominal value of g (9.81 m/s^2). Figure 8a shows the time history of the components (in the inertial frame) of the additional compensating control force to be applied to the center of mass C of body BR.

The control force is continuous as seen in Fig. 8b, where the timescale is expanded and a small portion of the time history of the compensating control force components on BR is shown from $t =$ 5 s to $t = 6$ s. Because the nominal control force at C on BR is zero, the total control force at C on BR is just the additional compensating control force shown in the figure.

Figure 9 shows the motion of the center of mass C of BR as well as the components of the quaternion vector $u(t)$. The dashed line in Fig. 9a represents the norm of the quaternion vector $u(t)$, which is seen to be unity throughout the integration interval. The error in satisfying the unit-quaternion constraint $e_u = u^T u - 1$ is of $O(10^{-11})$ throughout the interval of integration. Figure 9b shows the three components of the motion of the center of mass C of BR in the inertial frame.

To demonstrate that the compensating control forces are relatively insensitive to our estimate of the uncertainty in the actual system vis-à-vis the nominal system that is described by the value of the parameter β, we simulate the system again with a larger value of $\beta = \beta_1 = 10^{15}$, keeping the rest of the parameters unchanged. It should be noted that the new value β_1 for β is larger by a factor of 1000 than the earlier value β_0. Figure 10 shows plots for the additional compensating control forces on the discrete masses and the additional compensating torques with $\beta = \beta_1 = 10^{15}$, which can be compared with the corresponding plots for $\beta = \beta_0 = 10^{12}$ shown in Fig. 6. As seen from these figures, the compensating forces do not change perceptibly. The plot for the additional compensating control force at C on BR (not shown for brevity) also does not change perceptibly from that shown in Fig. 8. Thus, overestimating the uncertainties by using a value of β that is a 1000 times as large as previously, as might

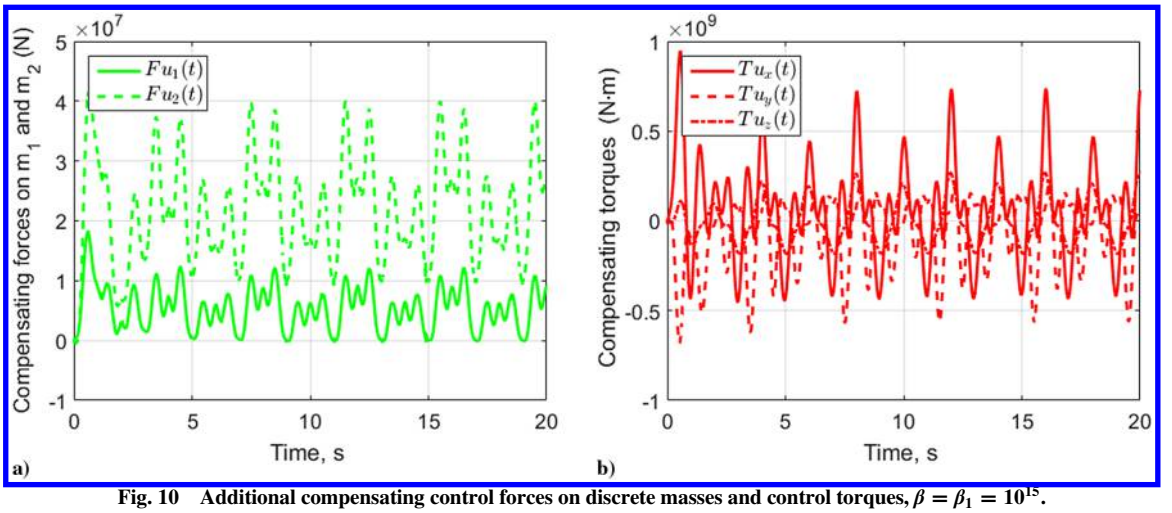

Fig. 10 Additional compensating control forces on discrete masses and control torques, $\beta = \beta_1 = 10^{15}$.

be done in practice from a conservative standpoint, does not cause much change in the (generalized) additional compensating control forces (see Result 3).

Comparing Figs. 3a, 4a, and 9b (which show the controlled response of the uncertain system) with Figs. 9a, 10a, and 11b, respectively, shown in [1] for the controlled response of the nominal system, we indeed observe that the uncertain system behaves as though it were the nominal system, devoid of uncertainty.

B. Example 2

As a second example, we consider a hollow cylinder B with a coaxial rod R along which a chain of five masses, connected together with nonlinear springs, can slide freely. The system is shown in Fig. 12. As with example 1, we first summarize the parameters of the nominal system followed by the parameters of the (realized) actual uncertain system.

1. *Nominal System*

The outer diameter of the cylinder is $D = 8$ m, its outer length is $h = 12$ m, the thickness of the wall is $a = 2$ cm, and the diameter of the rod is 20 cm. The cylinder and rod are made of steel with a density of 7×10^3 kg/m^3. The center of mass C of the body BR (cylinder + rod) is located along the axis of the cylinder at the center of the rod. The body fixed xyz frame has its x axis along the axis of the rod, and the other two body axes lie perpendicular to the axis of the rod. The mass of BR is $m_{BR,(n)} = 2.934 \times 10^4$ kg. Its moment of inertia matrix in the xyz body-fixed frame is $J_{(n)} = 10^5 \times \text{diag}(7.809, 7.535, 7.535)$ kg $\cdot$ m^2. The center of mass of the cylinder itself is taken as the reference point (it lies along the rod) O'; hence, vector $d = [0, 0, 0]^T$. The unit vector along the rod R is $a = [1, 0, 0]^T$. The equilibrium positions p_e of the discrete masses measured along R are uniformly spaced along its length, $h - 2a$. The nominal (constant) acceleration due to gravity is taken to be $g_{(n)} = 9.81$ m/s^2.

The masses that slide along the rod have values $m_{(n)} = 10^4 \times [1, 2, 2, 1, 1]^T$ kg. The stiffnesses of the linear spring elements connecting the masses are $k^l_{(n)} = [70, 50, 70, 100, 70, 50]^T$ mN/m, and nonlinear (cubic) stiffnesses are $k^n_{(n)} = [30, 70, 40, 60, 50, 80]^T$ kN/m^3.

The initial position of C in an inertial frame (with the inertial Z axis pointed upward) is taken to be the origin, so that $R(0) = [0, 0, 0]^T$, and its initial velocity is taken to be $\dot{R}(0) = [1, 2, 10]^T$ m/s. The cylinder is aligned so that its body-fixed x-axis lies along the inertial X axis. The initial orientation of the body is obtained by rotating it about the unit vector $\nu = 1/\sqrt{3}[1, 1, 1]^T$ in the inertial frame through an angle $\theta = \pi/3$ so that the initial quaternion is $u(0) = [\cos(\theta/2), \sin(\theta/2)\nu]^T$. The initial angular velocity in the body-fixed frame is taken to be the three-vector $[1, -1, 2]^T$ rad/s, so that $\dot{u}(0) = [-0.2887, 0.8660, -0.5477, 0.5774]^T$. The initial positions measured along R, relative to the reference point C of the five masses, are $p(0) = [-4.4, -1.8, 1.4, 2.5, 4.2]^T$ m; and their initial velocities are $\dot{p}(0) = [0.2, -0.3, -0.2, 0.1, -0.2]^T$ m/s. With these initial conditions, the body is allowed to undergo free gravitational fall.

2. *Actual System*

To demonstrate the control methodology, a specific actual system, picked from an ensemble of unknown systems, is described in the following.

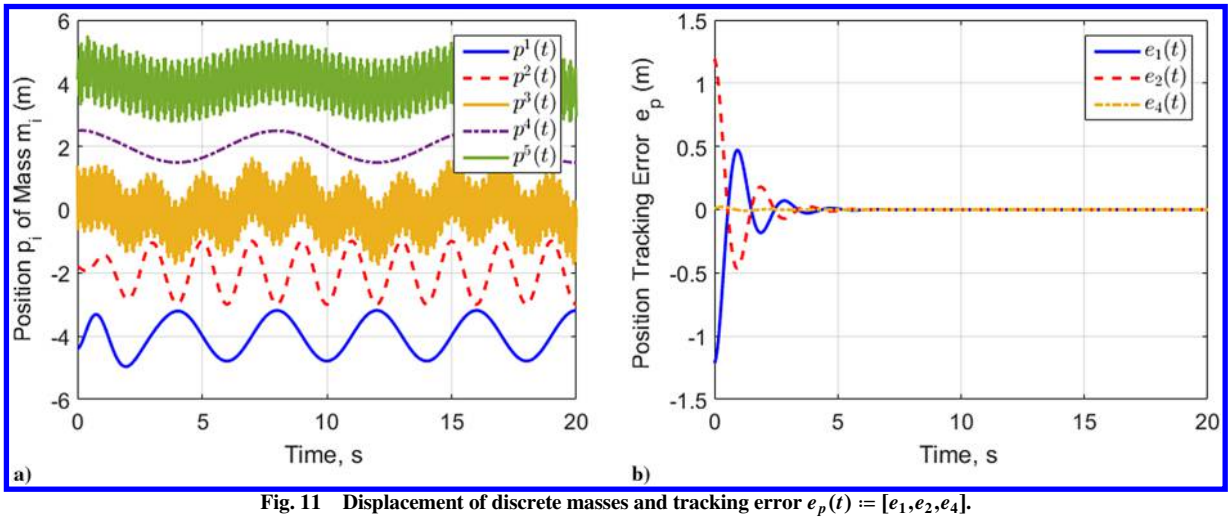

Fig. 11 Displacement of discrete masses and tracking error $e_p(t) := [e_1, e_2, e_4]$.

The mass of BR in the actual system is $m_{BR} = 2.86 \times 10^5$ kg. Its moment of inertia along the principal axes is $J = 10^5 \times \text{diag}(6.2649, 6.7889, 8.4262)$ kg $\cdot$ m^2. The actual masses of the sliding discrete masses are $m = 10^4 \times [0.903, 2.04, 2.042, 0.921, 0.976]^T$ kg. The linear spring elements connecting the masses have stiffnesses $k^l = [71.09, 50.96, 68.77, 101.56, 70.22, 50.48]^T$ mN/m, and the stiffnesses of the nonlinear cubic spring elements are $k^n = [30.781, 71.146, 36.164, 56.520, 50.447, 84.306]^T$ mN/m^3.

In summary, the mass of BR in the actual system differs from that used in the nominal system by approximately 2.5%, the maximum difference in the entries of the moment of inertia matrix of BR between the actual and the nominal system is about 20%, the values of the discrete masses differ by about 10%, the values of the stiffnesses of the linear spring elements differ by 2%, and the values of the stiffnesses of the cubic spring elements differ by 6%.

The gravitational constant is also assumed to be uncertain, and its actual value is taken to be $g = 9.73$ m/s^2.

3. Control Requirements

Similar to example 1, we control the angular velocity of the tumbling body and internal motions of the discrete masses so they track desired trajectories. However, we only control the positions of the first, second, and the fourth discrete masses. The desired position of these masses are

$$\bar{p}^i(t) = p_e^i + l^i \cos(\lambda_i t), \quad i = 1, 2, \text{ and } 4 \tag{60}$$

The desired angular velocity of the tumbling body is

$$\bar{\omega}_i(t) = b_i \cos(\sigma_i t), \quad i = 1, 2, \text{ and } 3 \tag{61}$$

For numerical simulation, the parameters are chosen to be

$$l^1 = 0.8, \quad l^2 = -1, \quad l^4 = 0.5; \quad \lambda_1 = \pi/2, \quad \lambda_2 = \pi, \quad \lambda_4 = \pi/4 \tag{62}$$

and

$$b = [8, -10, 15]^T \quad \text{and} \quad \sigma = [\pi, 0, 2\pi]^T \tag{63}$$

The parameters for the constraint matrices are chosen as

$$\alpha_i = 2, \quad \beta_i = 12, \quad i = 1, 2, 3 \tag{64}$$

$$\delta_1 = 0.5, \quad \delta_2 = 8, \quad \text{and} \quad \gamma = 0.4 \tag{65}$$

4. Compensating Controller

The parameters for the additional compensating control force are chosen as $\beta = \beta_0 = 0.5 \times 10^8$, $\varepsilon = 10^{-4}$ and $K = 3$. The tracking error bounds between the actual system and the nominal system using Eqs. (36) and (37) are

$$|e_i| \le \frac{1}{K}\varepsilon = 3.3 \times 10^{-5}, \quad i = 1, 2, \ldots, 12 \tag{66}$$

and

$$|\dot{e}_i| \le 2\varepsilon = 2 \times 10^{-4}, \quad i = 1, 2, \ldots, 12 \tag{67}$$

The equations of motion of the controlled uncertain system and the controlled nominal system given by Eqs. (17) and (1) are simultaneously integrated with the nominal control force and the compensating control force computed using Eqs. (16) and (25). Numerical integration is carried out using the ode15s package in MATLAB with a relative error tolerance of 10^{-10} and an absolute error tolerance of 10^{-12}. The results are presented in Figs. 11–20. Figure 11 shows the time history of the positions of the discrete masses relative to the reference point $C(O')$ of the controlled uncertain system as well as the errors in tracking the control requirements $e_p(t) = p(t) - \bar{p}(t)$. At the end of 20 s, the tracking error $e_p(20)$ is $O(10^{-9})$ m. If the numerical integration is continued until 60 s, the tracking error $e_p(60)$ is $O(10^{-11})$. Figure 13 shows the time history of various components of the angular velocity vector. It also shows the error in satisfying the control requirements $e_\omega(t) := \omega(t) - \bar{\omega}(t)$ imposed on the angular velocity of the uncertain body BR. At the end of 20 s, the error $e_\omega(20)$ is $O(10^{-3})$ rad/s; at the end of 60 s, the error $e_\omega(60)$ is $O(10^{-10})$ rad/s. Integration over longer time intervals gives errors of the same order of magnitude as the error tolerances used in the numerical integration.

The tracking error at the end of 60 s between the states of the nominal and the actual systems ($e = q - q_{(n)}$) is of $O(10^{-5})$, and the tracking error in the generalized velocity ($\dot{e} = \dot{q} - \dot{q}_{(n)}$) is of $O(10^{-4})$, as predicted by Eqs. (66) and (67).

Figure 14 shows the generalized nominal control force Q^C to be applied to the tumbling–vibrating body so that the nominal system satisfies the control requirements. Forces on the discrete masses are shown in Fig. 14a, whereas Fig. 14b shows the control torques to be applied to BR about its principal axes. No nominal force is applied at C to BR (computationally less than 10^{-20} N throughout the interval of integration). Because discrete masses m_3 and m_5 are not controlled, the nominal control forces applied to these two masses turn out to be zero. These plots can be compared with similar ones in Fig. 15 that show the generalized additional compensating control force Q^u. These additional generalized forces are much smaller than the generalized nominal forces. It is important to note that the compensating control force is smooth. Figures 16a and 16b show the additional compensating control forces on the discrete masses and the additional compensating control torques on an expanded timescale from $t = 5.5$ to

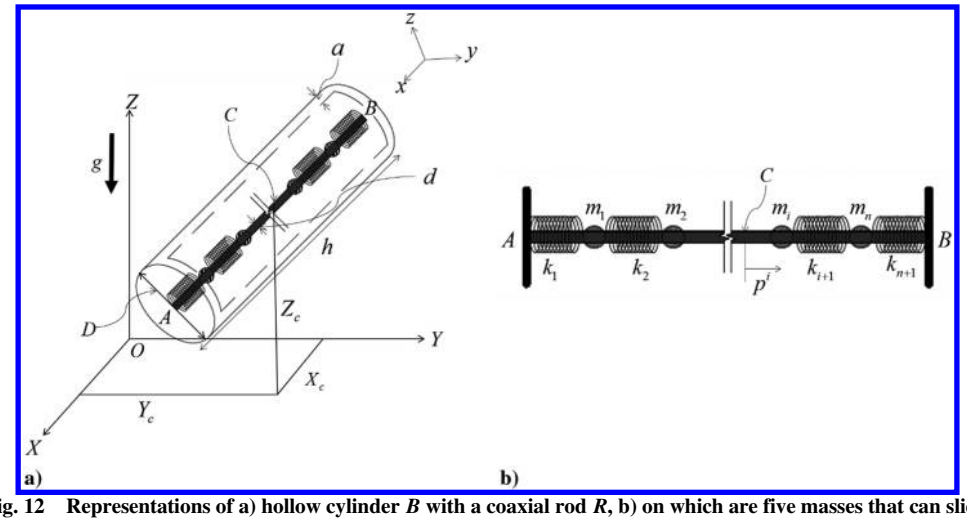

Fig. 12 Representations of a) hollow cylinder B with a coaxial rod R, b) on which are five masses that can slide.

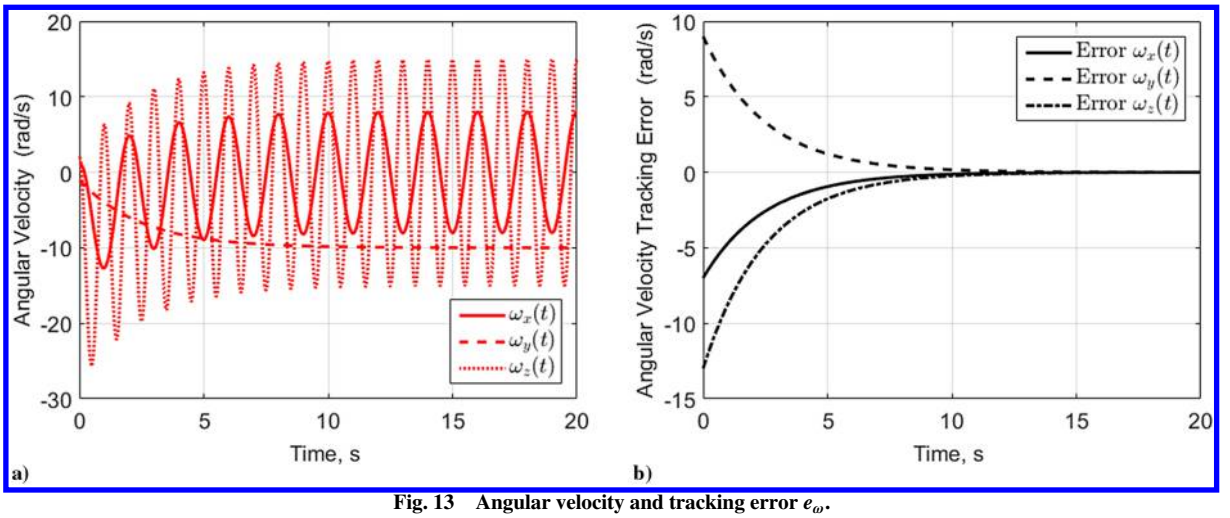

Fig. 13 Angular velocity and tracking error e_ω.

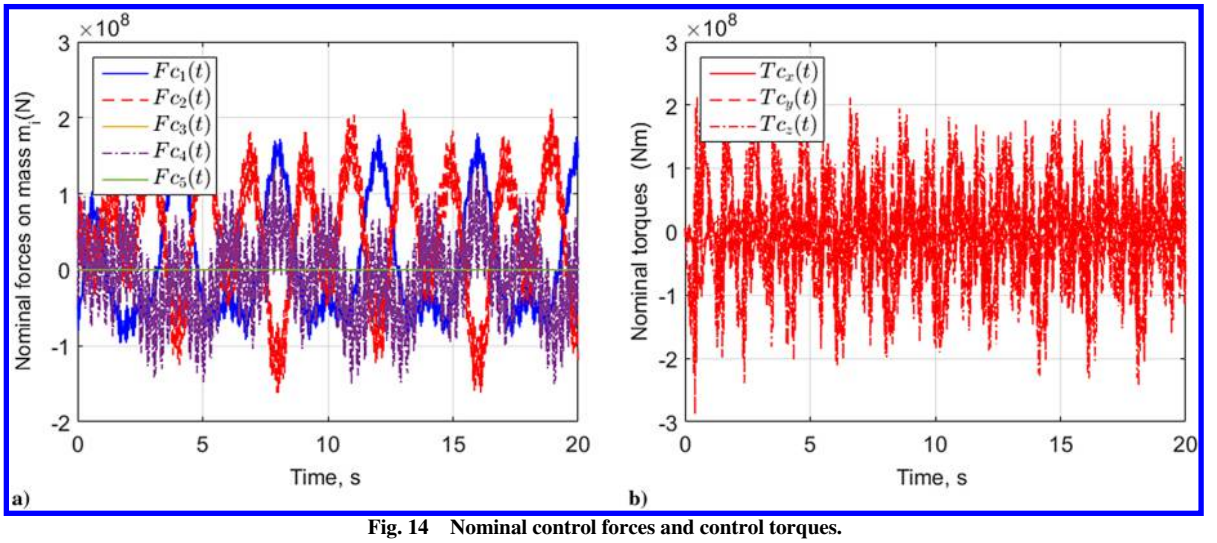

Fig. 14 Nominal control forces and control torques.

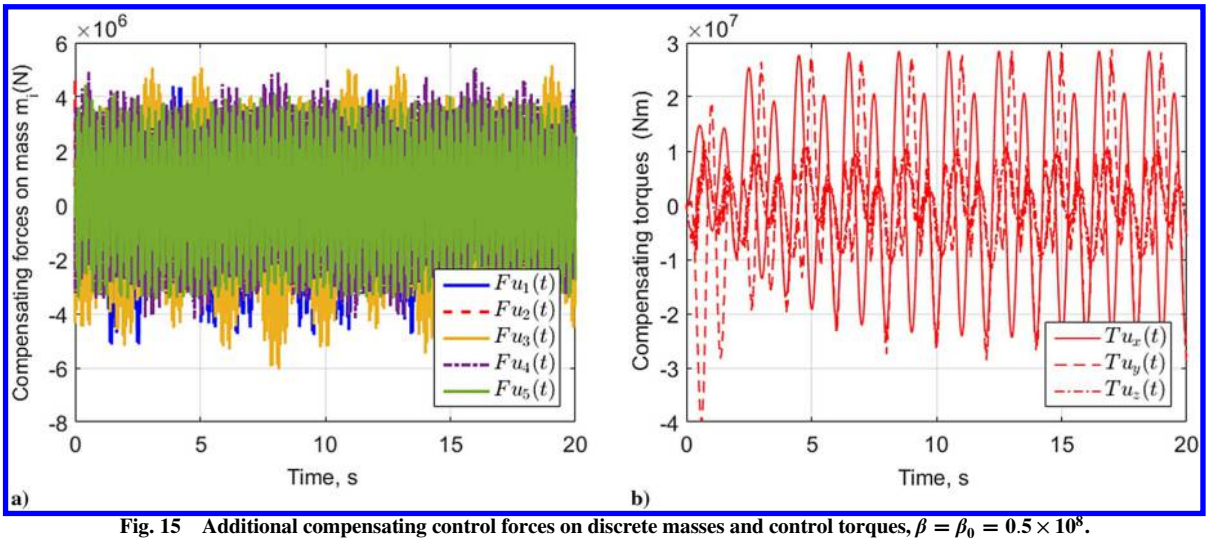

Fig. 15 Additional compensating control forces on discrete masses and control torques, $\beta = \beta_0 = 0.5 \times 10^8$.

$t = 6.0$ s. As seen in the figure, they are smooth functions of time. The figure also shows that, though no nominal control forces are applied to the discrete masses m_3 and m_5, there are additional compensating control forces on them.

Figure 17a shows the time history of the components (in the inertial frame) of the additional compensating control force applied to the center of mass C of BR. As before, the additional compensating control does not exhibit chattering, and Fig. 17b shows these components from $t = 5.5$ s to $t = 6$ s on an expanded scale. Because the nominal control force at C on BR is zero, the total control force at C on BR is just the additional compensating control force shown in the figure.

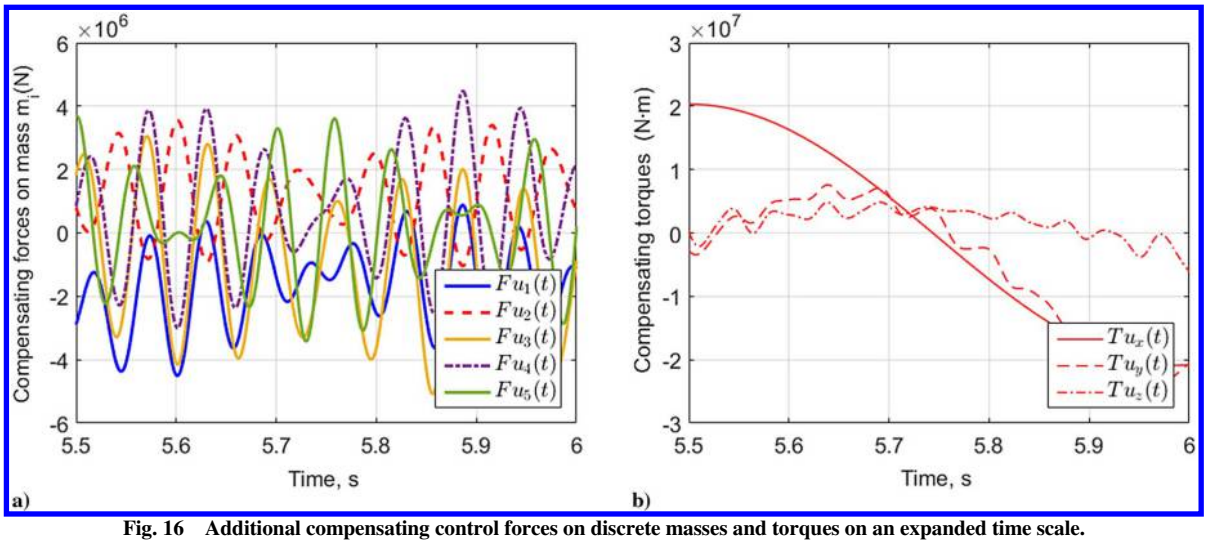

Fig. 16 Additional compensating control forces on discrete masses and torques on an expanded time scale.

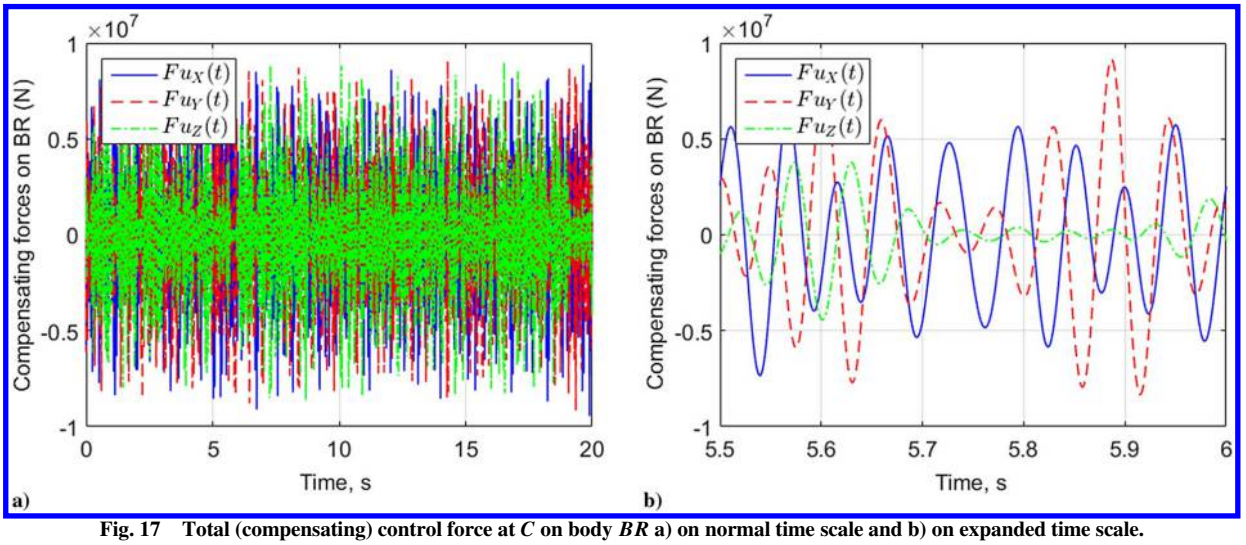

Fig. 17 Total (compensating) control force at C on body BR a) on normal time scale and b) on expanded time scale.

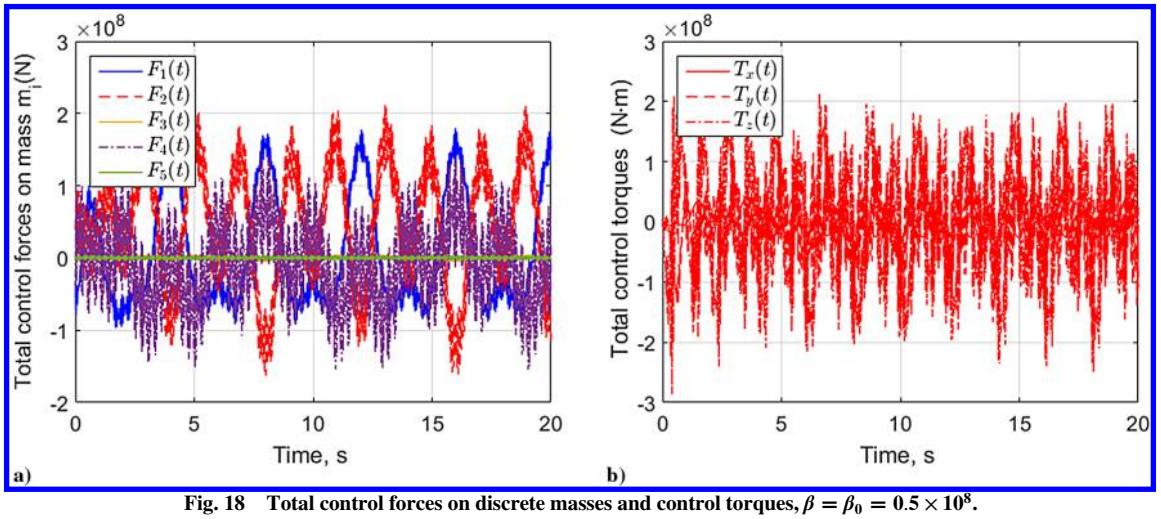

Fig. 18 Total control forces on discrete masses and control torques, $\beta = \beta_0 = 0.5 \times 10^8$.

Figure 18 shows the total control force $Q^C + Q^u$ applied to the five discrete masses and the torques applied to BR about its principal axes. As with example 1, the control forces on the discrete masses and the torques are seen to be much smaller than the nominal ones. The total generalized control force, consisting of the sum of the nominal and the compensating control force, when acting on the uncertain system causes it to exactly mimic the controlled nominal system, and therefore behave as though there were no uncertainty in the nominal description, thereby satisfying the control requirements.

Figure 19a shows the components of the quaternion vector $u(t)$. The error in satisfying the unit-quaternion constraint $e_u = u^T u - 1$ is of $O(10^{-6})$ throughout the interval of integration. Figure 19b shows the motion of the center of mass C of BR in the inertial frame.

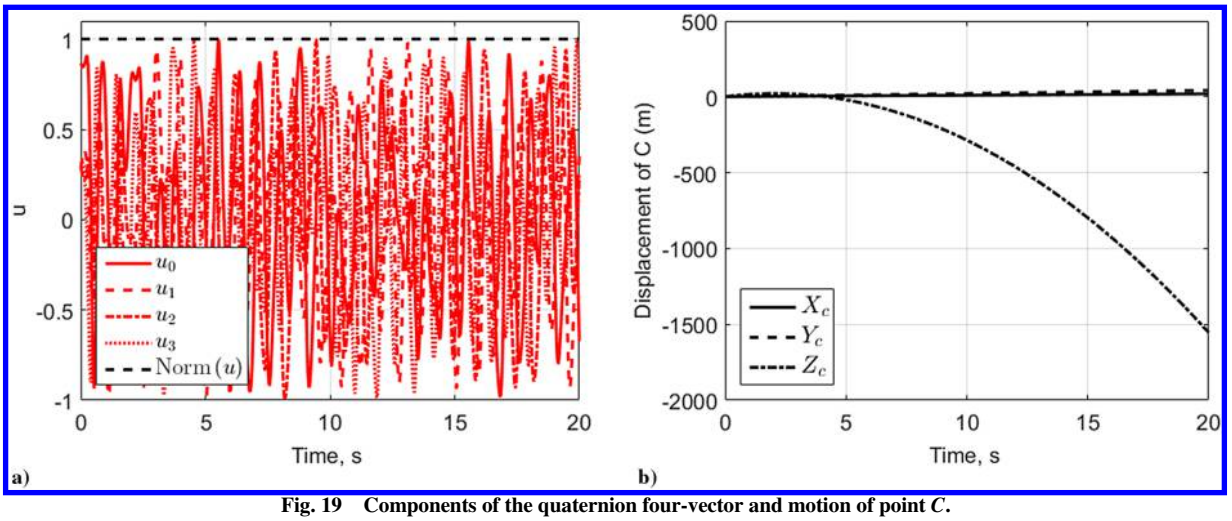

Fig. 19 Components of the quaternion four-vector and motion of point *C*.

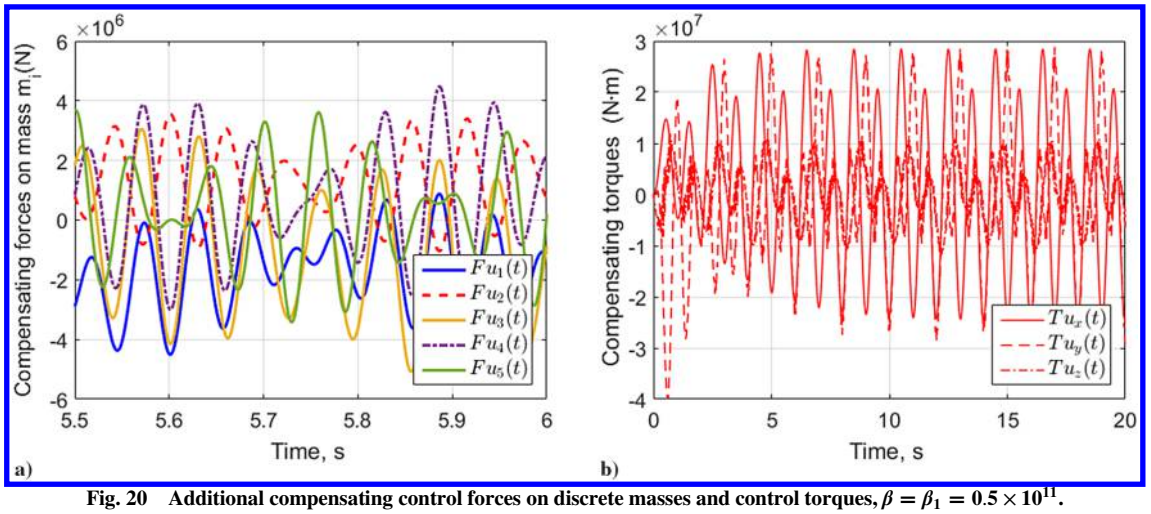

Fig. 20 Additional compensating control forces on discrete masses and control torques, $\beta = \beta_1 = 0.5 \times 10^{11}$.

We now assume that our guesstimate of the uncertainty β is in error by a factor of 1000. Figure 20 shows the additional compensating control forces obtained when the controlled uncertain cylinder system is simulated with a value of $\beta = \beta_1 = 0.5 \times 10^{11}$. A comparison of Figs. 16a and 20a shows that the additional compensating forces on the discrete masses when using a higher value of β (here, $\beta_1 = 1000\beta_0$) does not result in any significant change in the additional compensating control forces. A comparison of Figs. 15b and 20b shows a similar result for the additional compensating control torques. For brevity, we have not shown the additional compensating control force components acting at C on the body BR when $\beta_1 = 1000\beta_0$, but they look nearly identical to those shown in Figs. 17a and 17b.

Figures 11a, 13a, and 19b, showing the controlled response of the uncertain system, can be compared with figures 13a, 14a, and 16b of [1], which show the response of the controlled nominal system. The response time histories look exactly the same in both the cases, demonstrating that the controlled uncertain system behaves as though it were the nominal system, with no uncertainty in its description.

V. Conclusions

In this paper, a generic uncertain multibody system is considered with internal degrees of freedom that has practical significance in studying phenomena like liquid sloshing in rockets, capture and refurbishing of space debris, etc. It is assumed that the parameters describing the mathematical model of the system and the given forces acting on it are not accurately known, but their estimates are available, and so are the bounds on the extent to which the actual values might deviate from these estimates. A simple control strategy is used to effectively control the uncertain system such that the system tumbles in a desired fashion, whereas the internal degrees of freedom execute user-prescribed oscillatory motions. It is capable of being used for both autonomous and nonautonomous systems.

The control methodology consists of two steps: 1) the determination of the generalized control force on the nominal system (the best guess of the actual system) and 2) the determination of an additional control to compensate for the uncertainties in the description of the nominal system. The control obtained in the first step of the methodology ensures that the nominal system satisfies exactly the control requirements asymptotically, and this has been dealt with in detail in [1]. This nominal control force is obtained using results from analytical dynamics, and it minimizes a control cost at each instant of time. It is the second step of the methodology that this paper deals with.

The central idea here is to find an additional compensating control so that the uncertain system dynamically behaves in the same manner as the nominal system; that is, it behaves as though there is no uncertainty in the description of the nominal system. The (generalized) compensating control force is found so that the controlled actual system tracks the trajectories of the nominal system to within user-prescribed bounds. This is done through the use of a generalized sliding surface. The methodology relies on the use of a guesstimate of the uncertainties in our knowledge of the actual physical system and the forces acting on it vis-a-vis the nominal system that is used in the first step of the methodology.

The two-step approach developed herein is shown to be capable of delivering stable precision control of uncertain tumbling multibody systems using the full nonlinear dynamical description without any

linearizations and/or approximations. Yet, it is simple enough to be usable in real time. This is because the control forces are obtained in closed form, with negligible associated computational costs. Two examples illustrate the ease of implementation and simplicity of the methodology, as well as the high precision with which stable control of uncertain nonautonomous systems can be effected through this approach. Furthermore, the explicit closed-form control obtained using this methodology is shown to be relatively insensitive to our ignorance of the uncertainties involved, which is an aspect that has considerable significance when dealing with the precision control of real-life uncertain systems. This too is illustrated through the examples considered.

References

[1] Koganti, P. B., and Udwadia, F. E., "Dynamics and Precision Control of Tumbling Multibody Systems," *Journal of Guidance, Control, and Dynamics* (submitted for publication).

[2] Lizarralde, F., and Wen, J. T., "Attitude Control Without Angular Velocity Measurement: A Passivity Approach," *IEEE Transactions of Automatic Control*, Vol. 41, No. 3, 1996, pp. 468–472. doi:10.1109/9.486654

[3] Show, L.-F., Juang, J.-C., Lin, C.-T., and Jan, Y.-W., "Spacecraft Robust Attitude Tracking Design: PID Control Approach," *Proceedings of the American Control Conference*, IEEE, Piscataway, NJ, May 2002, pp. 1360–1365. doi:10.1109/ACC.2002.1023210

[4] Hu, Q., Ma, G., and Xie, L., "Robust and Adaptive Variable Structure Output Feedback Control of Uncertain Systems with Input Nonlinearity," *Automatica*, Vol. 44, No. 2, 2008, pp. 552–559. doi:10.1016/j.automatica.2007.06.024

[5] Yang, Y., Wu, J., and Zheng, W., "Variable Structure Attitude Control for an UAV with Parameter Uncertainty and External Disturbance," *Proceedia Engineering*, Vol. 15, 2011, pp. 408–415. doi:10.1016/j.proeng.2011.08.078

[6] Chen, M., and Wu, Q.-X., "Adaptive Neural Control for Uncertain Attitude Dynamics of Near-Space Vehicles with Oblique Wing," *Advances in Neural Networks–ISNN*, Vol. 2952, Lecture Notes in Computer Science, Springer, New York, 2013, pp. 196–203.

[7] Liu, H., "Quaternion-Based Robust Attitude Control for Uncertain Robotic Quadrotors," *IEEE Transactions on Industrial Informatics*, Vol. 11, No. 2, 2015, pp. 406–415. doi:10.1109/TII.2015.2397878

[8] Junkins, J. L., Akella, M. R., and Kurdila, A. J., "Adaptive Realization of Desired Constraint Stabilization Dynamics in the Control of Multibody Systems," *Philosophical Transactions of the Royal Society of London Series A: Mathematical and Physical Sciences*, Vol. 359, No. 1788, 2001, pp. 2231–2249. doi:10.1098/rsta.2001.0884

[9] Aghili, F., "A Prediction and Motion-Planning Scheme for Visually Guided Robotic Capturing of Free-Floating Tumbling Objects with Uncertain Dynamics," *IEEE Transactions on Robotics*, Vol. 28, No. 3, 2012, pp. 634–649. doi:10.1109/TRO.2011.2179581

[10] Udwadia, F. E., and Kalaba, R. E., "A New Perspective on Constrained Motion," *Proceedings of the Royal Society of London, Series A: Mathematical and Physical Sciences*, Vol. 439, Nov. 1992, pp. 407–410.

[11] Kalaba, R. E., and Udwadia, F. E., "Equations of Motion for Nonholonomic, Constrained Dynamical Systems via Gauss's Principle," *Journal of Applied Mechanics*, Vol. 60, No. 3, 1993, pp. 662–668. doi:10.1115/1.2900855

[12] Udwadia, F. E., "A New Perspective on the Tracking Control of Nonlinear Structural and Mechanical Systems," *Proceedings of the Royal Society of London, Series A: Mathematical and Physical Sciences*, Vol. 459, No. 2035, 2003, pp. 1783–1800. doi:10.1098/rspa.2002.1062

[13] Udwadia, F. E., "Optimal Tracking Control of Nonlinear Dynamical Systems," *Proceedings of the Royal Society of London, Series A: Mathematical and Physical Sciences*, Vol. 464, No. 2097, 2008, pp. 2341–2363. doi:10.1098/rspa.2008.0040

[14] Udwadia, F. E., and Koganti, P. B., "Optimal Stable Control for Nonlinear Dynamical Systems: An Analytical Dynamics Based Approach," *Nonlinear Dynamics*, Vol. 82, No. 1, 2015, pp. 547–562. doi:10.1007/s11071-015-2175-1

[15] Udwadia, F. E., and Wanichanon, T., "Control of Uncertain Nonlinear Multibody Mechanical Systems," *Journal of Applied Mechanics*, Vol. 81, No. 4, 2014, Paper 041020. doi:10.1115/1.4025399

[16] Udwadia, F. E., Koganti, P. B., Wanichanon, T., and Stipanovic, D., "Decentralized Control of Nonlinear Dynamical Systems," *International Journal of Control*, Vol. 87, No. 4, 2014, pp. 827–843.

[17] Udwadia, F. E., and Koganti, P. B., "Dynamics and Control of a Multi-Body Planar Pendulum," *Nonlinear Dynamics*, Vol. 81, No. 1, 2015, pp. 845–866. doi:10.1007/s11071-015-2034-0

[18] Utkin, V. I., *Sliding Modes and Their Application in Variable Structure Systems*, Mir Publ., Moscow, 1978, Chaps. 2, 3 (in English).

[19] Young, K. D., Utkin, V. I., and Özgüner, Ü., "A Control Engineer's Guide to Sliding Mode Control," *IEEE Transactions on Control Systems Technology*, Vol. 7, No. 3, 1999, pp. 328–342.

[20] Spurgeon, S. K., "Sliding Mode Observers: A Survey," *International Journal of Systems Science*, Vol. 39, No. 8, 2008, pp. 751–764. doi:10.1080/00207720701847638

[21] Levant, A., "Higher-Order Sliding Modes, Differentiation and Output-Feedback Control," *International Journal of Control*, Vol. 76, Nos. 9–10, 2003, pp. 924–941. doi:10.1080/0020404031000099029